



Contents lists available at ScienceDirect

Bioorganic & Medicinal Chemistry Letters

journal homepage: www.elsevier.com/locate/bmcl



Novel pyrrolo[2,1-*f*][1,2,4]triazin-4-amines: Dual inhibitors of EGFR and HER2 protein tyrosine kinases

Brian E. Fink^{*}, Derek Norris, Harold Mastalerz, Ping Chen, Bindu Goyal, Yufen Zhao, Soong-Hoon Kim, Gregory D. Vite, Francis Y. Lee, Hongjian Zhang, Simone Oppenheimer, John S. Tokarski, Tai W. Wong, Ashvinikumar V. Gavai

Department of Oncology Chemistry, Discovery Biology, Bristol-Myers Squibb Research and Development, PO Box 4000, Princeton, NJ 08543-4000, United States
Department of Computer Aided Drug Design, Bristol-Myers Squibb Research and Development, PO Box 4000, Princeton, NJ 08543-4000, United States

ARTICLE INFO

Article history:

Received 30 September 2010
Revised 18 November 2010
Accepted 22 November 2010
Available online 30 November 2010

Keywords:

EGFR
HER2
Kinase inhibitor

ABSTRACT

A novel series of 5-((4-aminopiperidin-1-yl)methyl)-pyrrolo[2,1-*f*][1,2,4]triazin-4-amines with small aniline substituents at the C4 position were optimized for dual EGFR and HER2 protein tyrosine kinase inhibition. Compound **81** exhibited promising oral efficacy in both EGFR and HER2-driven human tumor xenograft models.

© 2010 Elsevier Ltd. All rights reserved.

Receptor tyrosine kinases (RTK) play key roles in the processes governing cellular proliferation, differentiation and evasion from apoptosis. Among the known RTKs, the ErbB family, in particular EGFR and HER2 have been extensively studied and clinically validated as targets for cancer therapies.¹ The ErbB family consists of four receptors: epidermal growth factor receptor (EGFR/ErbB-1/HER1), HER2 (ErbB-2/neu), HER-3 and HER-4. Over-expression and/or constitutive activation of EGFR and HER2 have been observed in numerous tumor types, including colon, breast, ovarian, head and neck, and non-small cell lung cancers.² Current therapies using either monoclonal antibodies (cetuximab and trastuzumab) or small molecules (erlotinib) to selectively target EGFR or HER2, or more recently, small molecules that target both receptors (lapatinib), have demonstrated success in the clinic.³

We have previously reported the discovery and preclinical evaluation of [4-[[1-(3-fluorophenyl)methyl]-1*H*-indazol-5-ylamino]-5-methyl-pyrrolo[2,1-*f*][1,2,4]triazin-6-yl]-carbamic acid, (3*S*)-3-morpholinylmethyl ester (BMS-599626, **1**), as a selective and orally efficacious inhibitor of EGFR and HER2 kinases, culminating in our first entry into the clinic with a dual EGFR/HER2 inhibitor.⁴ Subsequently, the discovery and preclinical profiles of the C5-substituted pyrrolotriazines **2**⁵ and **3**⁶ have been disclosed. While **2** and **3** exhibited EGFR/HER2 biochemical potency comparable to that of **1**, the C5-substituted analogs showed dramatic improve-

ment in cellular potency in the HER2-overexpressing N87 gastric carcinoma cell line (Table 1). However, the increase in cellular activity did not result in substantially improved in vivo potency. Even though a five- to ten-fold improvement in anti-proliferative activity was seen, all three compounds were active in EGFR or HER2 driven in vivo tumor models in doses ranging from 60 to 180 mg/kg.^{4–6} Insufficient plasma exposure for **2** and **3** was thought to be the likely cause for the apparent lack of improvement in in vivo potency. Rapid disappearance of drug during pharmacokinetic profiling was observed in a mouse pharmacokinetic study for **2** and **3** relative to **1** (Table 1). It is likely that **2** and **3** do not maintain sufficient plasma concentrations to provide sustained inhibition of EGFR and HER2 for the period of time necessary for robust in vivo activity in tumor models.

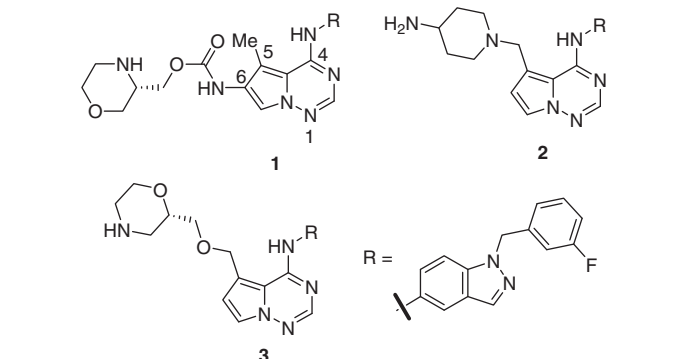
Here we describe our efforts to optimize the C5-substituted pyrrolotriazine series, focusing on reducing the molecular weight and overall lipophilicity as a means to improve the ADME properties and thereby improve exposure and in vivo potency.

A general synthetic approach was developed to allow for the rapid generation of C4 aniline SAR with a 4-aminopiperidinylmethyl or a morpholin-2-yl methoxymethyl group at the C5 position of the pyrrolotriazine (Scheme 1). 5-Methyl-4-(methylthio)pyrrolo[2,1-*f*][1,2,4]triazine **4**^{6,7} was reacted with *N*-bromosuccinimide (NBS) and catalytic benzoyl peroxide in carbon tetrachloride and the resulting 5-bromomethylpyrrolotriazine was treated with either (*S*)-*tert*-butyl 2-(hydroxymethyl)morpholine-4-carboxylate or *tert*-butyl piperidin-4-ylcarbamate to afford **5** or **6**, respectively. Oxidation of the C4 thiomethyl ether with *m*-CPBA, followed by

^{*} Corresponding author. Tel.: +1 609 252 3420.

E-mail address: brian.fink@bms.com (B.E. Fink).

Table 1
Pyrrolotriazine EGFR/HER2 inhibitors



	IC ₅₀ ^a (μM)			N87 MED ^c (mg/kg)	Mouse exposure ^d C _{max} /C _{4 h} (μM)
	EGFR	HER2	N87 ^b		
1	0.032	0.023	0.450	120	4.1/4.1
2	0.035	0.022	0.035	60	4.5/2.7
3	0.061	0.055	0.083	60	9.5/5.8

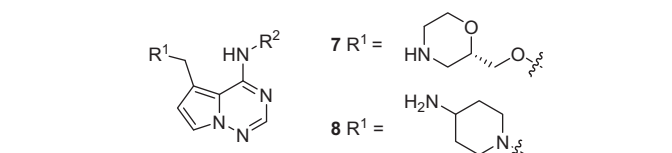
^a IC₅₀ values are reported as the mean of at least three determinations. Variability around the mean value was <15%.

^b N87 is a gastric tumor cell line (HER2⁺⁺⁺/EGFR⁺).

^c MED—minimum efficacious dose when dosed Q1D × 14, po. An active dose is defined as %tumor growth inhibition (TGI) >50%. Tumor cells were implanted subcutaneously in athymic mice and staged to approximately 100 mg prior to the initiation of drug therapy.

^d Average 4 h exposure in three male Balb/C mice for compounds administered orally at 50 mg/kg in Tween 80/PEG400/water (10/40/50).

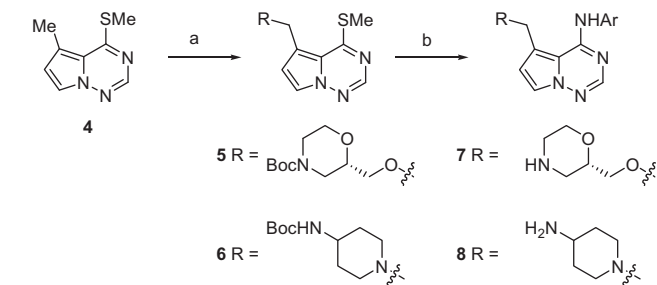
Table 2
Comparison of C5 amine substitutions



R ²	IC ₅₀ ^a (μM)			
	HER2	EGFR	N87	A2780 ^b
7a	>1.0	>1.0	NA	NA
8a	0.95	0.36	NA	NA
7b	0.67	0.02	4.4	3.9
8b	0.01	0.007	0.12	2.3
8c	0.04	0.009	0.14	3.7
8d	>1.0	0.88	NA	NA

^a IC₅₀ values are reported as the mean of at least three determinations. Variability around the mean value was <15%.

^b A2780 is an ovarian tumor cell line (HER2⁻/EGFR⁻).



Scheme 1. Reagents and conditions: (a) NBS (1.05 equiv), benzoyl peroxide (catalytic), CCl₄, N₂, reflux, 10 min, then (S)-tert-butyl 2-(hydroxymethyl)morpholine-4-carboxylate or tert-butyl piperidin-4-ylcarbamate (1.5 equiv), toluene, reflux, 55%; (b) m-CPBA (2.1 equiv), CH₂Cl₂, 0 °C to rt, 30 min; ArNH₂ (1.0 equiv), rt, 1–2 h; 15% TFA/CH₂Cl₂, 20–50%.

addition of an aniline and subsequent removal of the amine protecting group provided **7** or **8** in 20–50% yield.

Initial efforts to reduce the molecular weight and lipophilicity in the series focused on truncating the C4 *N*-benzylindazole (Table 2). Removal of the phenyl ring (**7a** and **8a**) resulted in significantly reduced biochemical potency against both HER2 and EGFR. These results were expected since previous SAR had suggested that HER2 potency in particular required the burying of a hydrophobic group deep into the ATP binding pocket. This had been suggested in a number of publications and corroborated by the published crystal structure of lapatinib bound to EGFR.^{8–11} Replacement of the entire *N*-benzylindazole of **3** with a *m*-acetylenic aniline (**7b**) resulted in the loss of HER2 activity while EGFR activity was maintained, again consistent with previous SAR. Surprisingly, when the same modification was made to compound **2**, the resulting analog (**8b**) demonstrated biochemical potency superior to either extended analog against both EGFR and HER2. Our results indicate that potent dual EGFR/HER2 inhibition is not dependent

on an extended hydrophobic motif at C4 and even a small aniline group at C4 is tolerated when optimal compensating interactions are identified at the C5 position.

A potential binding mode for **8b** in the ATP binding site was modeled using the published X-ray structure of the complex between erlotinib and the EGFR (Fig. 1).¹² In the model, the pyrrolotriazine core is oriented in the ATP binding site such that there is a hydrogen bond between N1 and the hinge region Met769 NH, serving to anchor and orient the pyrrolotriazine core in the ATP binding pocket. In this orientation, the C4 anilino group extends back into a hydrophobic pocket formed partially by the αC-helix beyond gatekeeper residue Thr766.

In our binding model, the C5 substituent is predicted to extend into the ribose-phosphate pocket where the piperidinyl amino group is available to participate in an extensive network of hydrogen bonds with the side chains of Asp831 and Asn818, and also with the backbone carbonyl oxygen of Arg817. Accessing this network of hydrogen bonding interactions within the ribose-phosphate pocket is hypothesized to more than compensate for any loss in binding energy associated with the reduction of hydrophobic non-bonded interactions when the C4 *N*-benzylindazole of **1** is replaced by a small aniline ring. Molecular modeling suggests the existence of an intramolecular hydrogen bond between the C4 aniline NH and the tertiary piperidinyl nitrogen, stabilizing the bioactive conformation depicted in Figure 1. Conformational analysis and molecular dynamics simulations with explicit waters indicate that the global energy minimum for **8b** is identical to the presumed bioactive conformation shown in Figure 1. These results are supported by small molecule X-ray structures for related analogs (data not shown) and through ¹H NMR studies where a significant downfield shift was observed for the C4 aniline NH, indicating a likely hydrogen bonding interaction with the tertiary piperidinyl nitrogen in solution.¹³ In contrast, while the morpholine nitrogen of **7b** may

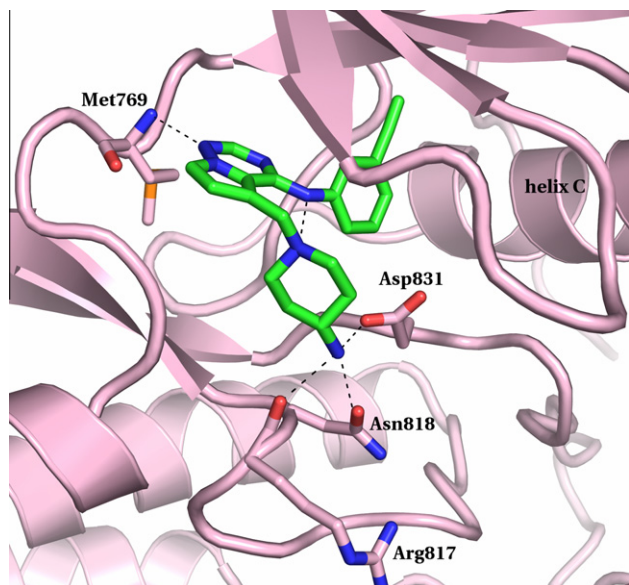


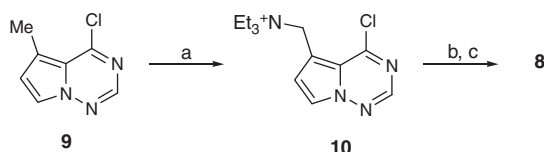
Figure 1. Predicted binding mode of **8b** in the X-ray structure of EGFR.¹²

also be positioned to take advantage of the network of hydrogen bonds in the ribose-pocket⁵, conformational analysis of **7b** shows a larger pool of low energy conformations other than the presumed bioactive conformation and the ¹H NMR chemical shift for the C4 aniline NH does not indicate an intramolecular hydrogen bond between the C4 aniline NH and the C5 alkoxymethyl group.¹³ These results suggest **7b** is not pre-organized to adopt the required bioactive conformation resulting in lower binding affinity for the morpholine-substituted analogs and establishing the aminopiperidine as an optimal C5 substituent for dual EGFR/HER2 activity.

Further modification of the C4 aniline demonstrated that an unsubstituted phenyl ring (**8c**) retained most of the biochemical activity in this series. Again, the strong network of interactions made between the 4-aminopiperidine group and the protein target serve to anchor the inhibitor in the binding pocket. Substitution of the C4 phenyl group with an aliphatic group (**8d**) was not tolerated and served to define the limits for binding to EGFR and HER2 at this position. Potent anti-proliferative activity was maintained in the HER2-driven N87 gastric carcinoma cell line for these truncated analogs. Importantly, minimal activity was observed in non-HER dependent tumor cell lines such as A2780, indicating that anti-proliferative effects of this series are dependent on EGFR/HER2 inhibition.

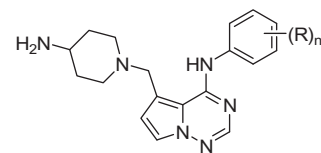
Having defined the minimum requirements for potent inhibition of EGFR and HER2 kinases in this series, further optimization of the aniline ring was investigated. Toward that end, an improved synthetic route was developed and is described in Scheme 2.^{5,6}

Pyrrolotriazine **9** was treated with NBS and catalytic benzoyl peroxide at reflux followed by reaction with triethylamine to afford the triethylammonium chloride **10**. Compound **10** was a



Scheme 2. Reagents and conditions: (a) NBS (1.05 equiv), benzoyl peroxide (catalytic), CCl₄, N₂, reflux, 10 min; Et₃N; 80%; (b) ArNH₂ (1.0 equiv), rt, 75–90%; (c) *tert*-butyl piperidin-4-ylcarbamate (1.5 equiv), toluene, reflux; 15% TFA/CH₂Cl₂; 63–95%.

Table 3
C4 Aniline SAR



	R	IC ₅₀ ^a (μM)			
		HER2	EGFR	N87	A2780
8e	2-Me	0.66	0.02	3.30	>5
8f	3-Me	0.02	0.005	0.14	>5
8g	4-Me	0.05	0.006	0.79	>5
8h	3-F	0.032	0.006	0.28	>5
8i	3-Cl	0.009	0.004	0.06	>5
8j	3-Br	0.006	0.004	0.05	2.6
8k	3-Cl, 5-Cl	0.13	0.034	3.36	4.0
8l	3-Cl, 4-F	0.01	0.006	0.12	>5
8m	3-Cl, 4-OMe	0.21	0.07	1.21	>5

^a IC₅₀ values are reported as the mean of at least three determinations. Variability around the mean value was <15%.

versatile intermediate for further SAR development since it is air stable and can be stored for extended periods of time without appreciable decomposition. Aromatic amines were added selectively to the C4 position allowing for the subsequent introduction of aliphatic amines at the C5 position, either stepwise or in a one-pot procedure.

Introduction of a methyl group around the C4 aniline ring (Table 3) identified the *m*-, and *p*-positions as most tolerant of substitution with respect to biochemical potency, while *o*-substitution resulted in a significant loss of activity (**8e**). This likely arises from increased steric interactions between the *o*-substituent and the pyrrolotriazine core forcing the aniline ring to adopt a less than optimal geometry in the binding pocket. That the loss in activity is more pronounced relative to HER2 than HER1 may be the result of a single residue difference between HER1 (Cys775) and HER2 (Ser783) in this region of the ATP binding pocket. It has been suggested that a strong network of water-mediated hydrogen bonds involving Ser783 in HER2 substantially impacts the structural requirements for inhibitor binding.¹⁴ Among the *m*- and *p*-substitutions (**8f** vs **8g**), the *m*-substituted analogs were favored by a factor of 2–3 which also translated into better cellular activity (0.14 vs 0.79 μM). Further

Table 4
Profile of lead dual HER2/EGFR inhibitors

	IC ₅₀ ^a (μM)			GEO MED (mg/kg)
	HER2	EGFR	N87	
1	0.03	0.020	0.42	120
8b	0.01	0.007	0.12	15
8f	0.02	0.005	0.14	60
8i	0.01	0.004	0.06	60
8l	0.01	0.006	0.12	15

^a IC₅₀ values are reported as the mean of at least three determinations. Variability around the mean value was <15%.

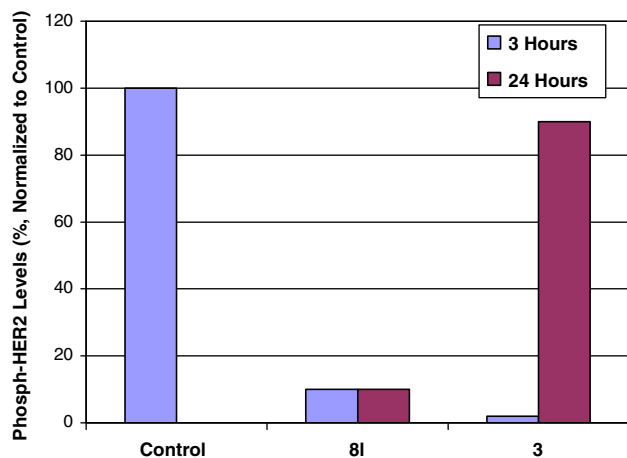
Table 5
Kinase selectivity profile for compound **8l**

Kinase	Fold selectivity versus HER2
BTK, JAK2, JAK3, KDR, Lck, PKCδ, PKCθ, Flt3	>10
PKCα, CDK2, FGFR, Met, GSK3β, CAMKII, IKK2, IGF-1R, IRAK4, AurA, MK2, p38α, CK1A1, IKK2, InsR, PLK1, SRC	>100

Table 6

Profile of lead compounds in N87 tumor model

Compound	N87 MED (mg/kg)	24 h exposure ^a			
		Dose (mg/kg)	C ₃ h (μM)	C ₂₄ h (μM)	AUC _{0–24} h (μM h)
3	60	240	5.8	0.1	100
8i	<15	15	7.2	6.8	160

^a Mean 24 h serum exposure in three male Balb/C mice for compounds administered orally in Tween 80/PEG400/water (10/40/50).**Figure 2.** Pharmacodynamic analysis of N87 tumors at 3 and 24 h after 21 days of dosing (**8i** = 15 mg/kg, **3** = 240 mg/kg). Each sample represents the pooling of three individual tumor samples.¹⁶

exploration of the *m*-position (**8h–8j**) showed that small hydrophobic substitutions were more potent and demonstrated corresponding improvements in cellular anti-proliferative activity. Compound **8i** was of particular interest, demonstrating extremely potent activity in N87 cells (IC₅₀ = 60 nM) while showing no observable potency in HER2/EGFR independent A2780 tumor cells (IC₅₀ >5000 nM).

Di-substitution on the C4 aniline ring was found to parallel the SAR developed for mono-substitution. The *m*- and *p*-positions were tolerant of substitution (**8i**) although increases in either steric bulk or polarity at the *p*-position resulted in decreased biochemical potency (**8m**). Other substitution patterns, such as 3,5-disubstitution, resulted in a substantial decrease in biochemical potency (**8k**).

Potential lead candidates were evaluated *in vivo* in the EGFR-driven GEO colon tumor xenograft model (Table 4). The rapid growth kinetics associated with the GEO xenografts allowed for rapid screening of compounds using an abbreviated 10-days dosing schedule. All compounds showed robust *in vivo* activity in the GEO model at minimum efficacious doses ranging from 15 to 60 mg/kg. Initial lead **8b** demonstrated good efficacy at doses as low as 15 mg/kg, however it was accompanied by significant weight loss, perhaps related to an undetermined off-target activity. Compound **8i**, among the most potent in the N87 cellular assay, provided lower than expected potency *in vivo* that was attributed to poor serum exposure. Compound **8i** showed *in vivo* potency superior to the previous lead **1**, and was selected for further evaluation.

Anti-tumor activity for compound **8i** in the N87 gastric cancer xenograft model was even more impressive (Table 6). Compound **8i** (MED <15 mg/kg) was over four-fold more potent than **3** (MED = 60 mg/kg). Pharmacokinetic analysis of drug exposure in serum over 24 h in Balb/C mice showed that **8i** had comparable drug exposure levels to **3**, but at a fraction of the dose (15 mg/kg vs 240 mg/kg).¹⁵ Clearly, improving the pharmacokinetic profile through reducing molecular size and lipophilicity resulted in

improved *in vivo* potency. A comparison of drug concentration at the 3 and 24 h time points shows that while both compounds show similar plasma concentrations at 3 h, at 24 h the concentration of **8i** remains significantly higher.

In addition, analysis of N87 tumor lysates using a phospho-HER2 endpoint demonstrated that **8i** suppressed HER2 signaling for a much longer period of time relative to **3** (Fig. 2), consistent with the observed improvements in pharmacokinetics and *in vivo* potency.

Compound **8i** showed a good level of kinase selectivity in a panel of diverse protein kinases (Table 5). Among the more potent off-target activities were Lck (IC₅₀ = 0.37 μM) and KDR (IC₅₀ = 0.11 μM), however, a 10-fold window was achieved against these important kinases. Greater than 100-fold selectivity was achieved versus a number of other receptor tyrosine kinases such as IGF-1R as well as serine/threonine kinases such as CDK2.

In summary, we have identified the C5 aminopiperidine as an important contributor to intrinsic potency of pyrrolotriazines against both HER2 and EGFR kinases. This substitution allows modification of the C4 position to reduce the overall size and lipophilicity leading to higher exposures and greatly improved *in vivo* potency in both HER2 (N87) and EGFR (GEO)-driven tumor models.

References and notes

- (a) Hynes, N. E.; Lane, H. A. *Nat. Rev. Cancer* **2005**, *5*, 341; (b) Baselga, J.; Arteaga, C. L. *J. Clin. Oncol.* **2005**, *23*, 2445.
- Salomon, D. S.; Brandt, R.; Ciardiello, F.; Normanno, N. *Crit. Rev. Oncol. Hematol.* **1995**, *19*, 183.
- Moy, B.; Kirkpatrick, P.; Kar, S.; Goss, P. *Nat. Rev. Drug Disc.* **2007**, *6*, 431.
- (a) Wong, T. W.; Lee, F. Y.; Yu, C.; Luo, F. R.; Oppenheimer, S.; Zhang, H.; Smykla, R. A.; Mastalerz, H.; Fink, B. E.; Hunt, J. T.; Gava, A. V.; Vite, G. D. *Clin. Cancer Res.* **2006**, *12*, 6186; (b) Gava, A. V.; Fink, B. E.; Fairfax, D. J.; Martin, G. S.; Rossiter, L. M.; Holst, C. L.; Kim, S.-H.; Leavitt, K. J.; Mastalerz, H.; Han, W.-C.; Norris, D.; Goyal, B.; Swaminathan, S.; Patel, B.; Mathur, A.; Vyas, D. M.; Tokarski, J. S.; Yu, C.; Oppenheimer, S.; Zhang, H.; Marathe, P.; Fargnoli, J.; Lee, F. Y.; Wong, T. W.; Vite, G. D. *J. Med. Chem.* **2009**, *52*, 6527.
- Mastalerz, H.; Chang, M.; Chen, P.; Fink, B. E.; Gava, A.; Han, W.-C.; Johnson, W.; Langley, D.; Lee, F. Y.; Leavitt, K.; Marathe, P.; Norris, D.; Oppenheimer, S.; Slecza, B.; Tarrant, J.; Tokarski, J. S.; Vite, G. D.; Vyas, D. M.; Wong, H.; Wong, T. W.; Zhang, H.; Zhang, G. *Bioorg. Med. Chem. Lett.* **2007**, *17*, 4947.
- (a) Mastalerz, H.; Chang, M.; Chen, P.; Dextraze, P.; Fink, B. E.; Gava, A.; Goyal, B.; Han, W.-C.; Johnson, W.; Langley, D.; Lee, F. Y.; Marathe, P.; Mathur, A.; Oppenheimer, S.; Ruediger, E.; Tarrant, J.; Tokarski, J. S.; Vite, G. D.; Vyas, D. M.; Wong, H.; Wong, T. W.; Zhang, H.; Zhang, G. *Bioorg. Med. Chem. Lett.* **2007**, *17*, 2036; (b) Gava, A. V.; Han, W.-C.; Chen, P.; Ruediger, E. H.; Mastalerz, H.; Fink, B. E.; Norris, D. J. *PCT Int. Appl. WO 2005065266*, 2005; 83.
- Mastalerz, H.; Chang, M.; Gava, A.; Johnson, W.; Langley, D.; Lee, F. Y.; Marathe, P.; Mathur, A.; Oppenheimer, S.; Tarrant, J.; Tokarski, J. S.; Vite, G. D.; Vyas, D. M.; Wong, H.; Wong, T. W.; Zhang, H.; Zhang, G. *Bioorg. Med. Chem. Lett.* **2007**, *17*, 2828.
- Fink, B.; Vite, G. D.; Mastalerz, H.; Kadow, J.; Kim, S.-H.; Leavitt, K.; Du, K.; Crews, D.; Mitt, T.; Wong, T.-W.; Hunt, J.; Vyas, D.; Tokarski, J. *Bioorg. Med. Chem. Lett.* **2005**, *15*, 4774.
- Cockerill, S.; Stubberfield, C.; Stables, J.; Carter, M.; Guntrip, S.; Smith, K.; McKeown, S.; Shaw, R.; Topley, P.; Thomsen, L.; Affleck, K.; Jowett, A.; Hayes, D.; Willson, M.; Woolard, P.; Spalding, D. *Bioorg. Med. Chem. Lett.* **2001**, *11*, 1401.
- Rusnak, D. W.; Affleck, K.; Cockerill, S. G.; Stubberfield, C.; Harris, R.; Page, M.; Smith, K. J.; Guntrip, S. B.; Carter, M. C.; Shaw, R. J.; Jowett, A.; Stables, J.; Topley, P.; Wood, E. R.; Brignola, P. S.; Kadwell, S. H.; Reep, B. R.; Mullin, R. J.; Alligood, K. J.; Keith, B. R.; Crosby, R. M.; Murray, D. M.; Knight, W. B.; Gilmer, T. M.; Lackey, K. *Cancer Res.* **2001**, *61*, 7196.

11. Wood, E. R.; Truesdale, A. T.; McDonald, O. B.; Yuan, D.; Hassel, A.; Dickerson, S. H.; Ellis, B.; Pennisi, C.; Horne, E.; Lackey, K.; Alligood, K. J.; Rusnak, D. W.; Gilmer, T. M.; Shewchuk, L. *Cancer Res.* **2004**, *64*, 6652.
12. Stamos, J.; Slikowski, C.; Eigenbrot, C. *J. Biol. Chem.* **2002**, *277*, 46,265. Molsoft modeling software was used to produce this figure. Molsoft LLC, 3366 No. Torrey Pines Ct., Ste. 300, La Jolla, CA 92037.
13. Compound **8b**: ^1H NMR (400 MHz, DMSO- d_6) δ 11.9 (s, 1H, NH); **7b**: ^1H NMR (400 MHz, DMSO- d_6) δ 9.6 (s, 1H, NH).
14. Bhattacharya, S. K.; Cox, E. D.; Kath, J. C.; Mathiowetz, A. M.; Morris, J.; Moyer, J. D.; Pustilnik, L. R.; Rafidi, D. T.; Su, C.; Wessel, M. D. *Biochem. Biophys. Res. Commun.* **2003**, *307*, 267.
15. The free fraction (fu) for **8l** and **3** were 1.2% and 2.6%, respectively, as determined by equilibrium dialysis at 10 μM .
16. Tumors were excised and homogenized in a glass homogenizer using a buffer that contained 1% Triton X-100, 40 mM Tris-HCl (pH 7.7), 10% glycerol, 1 mM EDTA, 0.15 M NaCl, 1 mM sodium vanadate, and 40 μM ammonium molybdate. Tumor lysates were centrifuged at 12,000 $\times g$ for 10 min and the supernatants were saved. Since the HER2 gene is amplified in N87 tumors, receptor phosphorylation was readily quantitated by western blot analyzes using tumor lysates directly. Tumor lysates (50 μg proteins) were fractionated by gel electrophoresis and western blot analysis was carried out using anti-phosphotyrosine antibody (PY20, Invitrogen), and anti-HER2 antibody (see Ref. 4b). HER2 receptor phosphorylation was quantified by densitometry and normalized against HER2 receptor levels.